Biochemical Pharmacology, Vol. 40, No. 1, pp. 89–96, 1990.
Printed in Great Britain.

0006-2952/90 $3.00 + 0.00

TWO-DIMENSIONAL NMR STUDY OF A PROTEIN–DNA COMPLEX

lac REPRESSOR HEADPIECE–OPERATOR INTERACTION

ROBERT KAPTEIN,* ROLF M. J. N. LAMERICHS, ROLF BOELENS and J. ANTON C. RULLMANN
Department of Chemistry, University of Utrecht, Padualaan 8, 3584 CH Utrecht, The Netherlands

Abstract—The interaction of the N-terminal DNA-binding domain (56 amino acid residues) of the *lac* repressor with *lac* operator DNA was analyzed using two-dimensional NMR spectroscopy. Both half-operators (11 and 14 bp) and a complete fully symmetric 22 bp operator were studied. Two-dimensional nuclear Overhauser effect (2D NOE) spectra of headpiece–operator complexes were taken in both D_2O and H_2O solutions. Special attention was given to the problem of ^1H resonance assignments. Based on an analysis of the proton–proton NOEs, a model for the headpiece–operator complex could be derived. In this model, most of the protein–DNA contacts occur between amino acid residues in the second helix (recognition helix) of the *lac* headpiece and DNA bases in the major groove. The orientation of this helix with respect to the dyad axis of the operator is opposite to that found in the X-ray structures of several other repressor–operator complexes.

The regulation of gene expression often occurs at the level of the initiation of transcription and involves tho binding of regulatory proteins to their DNA target sites. For this reason the specificity of protein–DNA interaction constitutes an important problem in molecular biology. Recently, results from X-ray crystallography and NMR spectroscopy have shed some light on the structures of protein–nucleic acid complexes, but the general problem of protein–DNA recognition is still far from being solved.

It was realized early that individual base pairs in double-stranded DNA can be discriminated by a combination of complementary hydrogen bonding and hydrophobic interactions with the thymine methyl groups [1, 2]. These general ideas have been confirmed to a large extent by the recent crystal structures of complexes of λ repressors [3] and 434 repressor [4] and cro [5] with their respective operator fragments. In these structures, base pairs indeed interact with amino acid side chains through hydrogen bonds and hydrophobic interactions. In addition, extensive networks of hydrogen bonds occur involving the sugar-phosphate DNA backbone. However, these and other studies also led to new notions about what confers specificity in protein–DNA interaction. In the 434 operators, there is a preference for AT or TA base pairs in the center of the operator where no contacts with the repressor occur [6]. These base pairs are apparently required for a correct positioning of the monomers of the dimeric repressor on the DNA. A more pronounced example of the role of sequence-dependent DNA structure or flexibility was found for the *trp* repressor–operator complex [7]. Here, a major part of the specificity is assumed to be due to a so-called indirect read-out mechanism [7], meaning that sequence-dependent DNA conformations, either pre-existing or protein-induced, allow the protein to make hydrogen bonds with the sugar-phosphate backbone. Surprisingly, in the *trp* repressor–operator complex direct hydrogen bonds between bases and amino acid chains are absent, and hydrogen bonding occurs only indirectly via water molecules. How well these water mediated H-bonds can serve in specific recognition is not yet clear, however.

All these proteins contain a particular substructure called helix-turn-helix motif first found in the early 1980s in the X-ray structures of the catabolite gene activating protein (CAP) [8], and the phage λ proteins cI (or λ) repressor [9] and cro repressor [10]. The second helix of this motif (the recognition helix) contains most of the determinants for specific DNA recognition. It was later shown by NMR spectroscopy that the *Escherichia coli lac* repressor is also a member of the family of helix-turn-helix proteins [11, 12]. The N-terminal DNA-binding domain (or headpiece) of the *lac* repressor was in fact one of the first proteins, the structure of which was determined solely by NMR spectroscopy [12, 13]. It contains three α-helices, the first two in the peptide region 6–25 constituting the helix-turn-helix motif. Recent work of our group has focused on the interaction of the *lac* headpiece containing 56 amino acid residues (HP56) with various *lac* operator fragments. The wild type *lac* operator has partial palindromic symmetry (see Fig. 1) and binds two headpiece domains of the repressor. The initial work was done with a 14 bp operator half site. A two-dimensional (2D) NMR study of the 1:1 complex with HP56 identified a number of protein–DNA "contacts" from nuclear Overhauser effects (NOEs) and the first low resolution model of the complex could be constructed [14]. An interesting result of this work was that the orientation of the helix-turn-helix domain of the headpiece with respect to the dyad axis of the operator was opposite to that found in all repressor–

* Author to whom correspondence should be addressed.

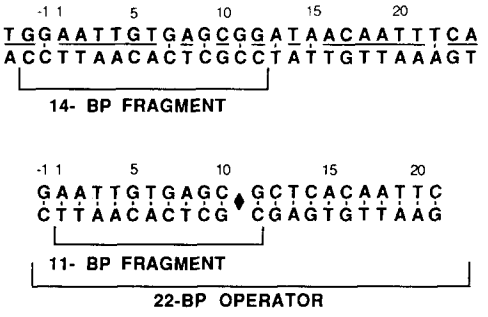

Fig. 1. Sequence of native *lac* operator (top) and "ideal" symmetric *lac* operator (bottom). Synthetic operator fragments of 11, 14, and 22 bp used in the NMR studies are indicated.

operator complexes studied by X-ray crystallography. This was later confirmed in a study on a 22 bp fully symmetric operator (cf. Fig. 1) with two headpieces bound [15]. Recent results of genetic experments on the *lac* system [16] have shown that this is not just a property of the isolated headpiece, but that the intact repressor makes use of the same binding mode.

In this paper we shall discuss the 2D NMR work on *lac* headpiece–operator complexes. Whereas the previous work was based on 2D NOE spectra recorded in D_2O solution, we shall focus here on spectra taken in H_2O. It was found that an 11 bp half site is the minimum length for an operator that still binds HP56 with sufficient affinity and specificity.

Assignment strategies

The total molecular weight of the HP56–11 bp operator complex is *ca.* 13 kD, and the formidable complexity of the spectra taken in H_2O requires a special consideration of the problem of ^1H resonance assignments. Combined use of the following strategies was made: (i) sequential assignment of both protein and DNA, (ii) comparison of free species, and (iii) titrations (varying the ratio of headpiece-to-operator and salt concentration). Upon forming the complex between headpiece and operator fragments, chemical shift differences occur with respect to the free species, but these are rarely larger than 0.1 to 0.2 ppm, and only observed for protons in or near the protein–DNA interface. Actually, the fact that internal residues in the protein such as Tyr 47, Leu 6 and Val 9 with characteristic shifts, quite different from their random coil positions, hardly shift upon complex formation is an indication that the basic folded structure of the headpiece does not change upon operator binding. Thus, in comparing 2D homonuclear Hartmann–Hahn (HOHAHA) and 2D NOE spectra of the complex with those of the free headpiece, similar patterns of cross-peaks can be detected, which are a great help in the assignment.

Another important feature is the fact that the complex is in fast exchange with the free constituents. This is true for almost all resonances except for a few which show the largest shift difference and are broadened in the complex. Unfortunately, these are also among the most interesting ones as they are in

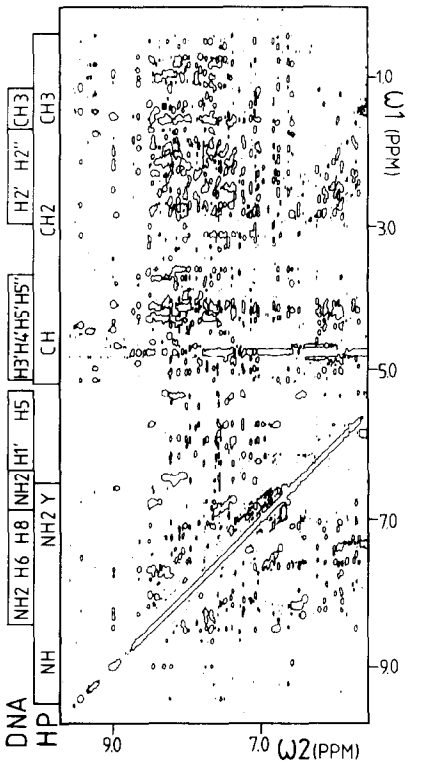

Fig. 2. Expanded region from $\omega_2 = 5.51$ to 9.67 ppm and $\omega_1 = 0.08$ to 9.67 ppm of a ^1H 2D NOE spectrum of the complex between HP56 and the 11 bp half-operator in ^1H_2O recorded at 600 MHz. Indicated are the regions where the protons of protein and the DNA resonate. This part of the spectrum contains the amide proton resonances of the headpiece which are essential for the sequential assignment. The spectrum is the sum of 2D NOE spectra recorded with mixing times of 125 and 250 msec respectively.

the interface region. For instance, we have not been able to detect the backbone amide proton of Gln 18 in the complex, presumably due to severe broadening. The exchange behavior is further complicated by the fact that, apart from the specific complex, non-specific complexes are also formed. Their contribution can be reduced, however, by working at *ca.* 0.2 M salt, using the fact that the non-specific interaction has a stronger ionic strength dependence than the specific one. The fast exchange situation allows one to connect the resonance positions in the complex with those of the free species by carrying out a series of 2D NMR experiments at various ratios of headpiece to operator concentrations. This can also be accomplished by taking a series of 2D NMR spectra at various salt concentrations in the range of 0.2 to 1.2 M. Protein–DNA complexes generally dissociate at high salt concentration due to the strong electrostatic component to the binding energy. These properties can be exploited in conjunction with the standard procedures for making sequential resonance assignments for proteins [17] and DNA fragments [18, 19].

Assignment of headpiece protons in the complex. Figure 2 shows the amide proton-region of the 600 MHz 2D NOE spectrum of the HP56–11 bp

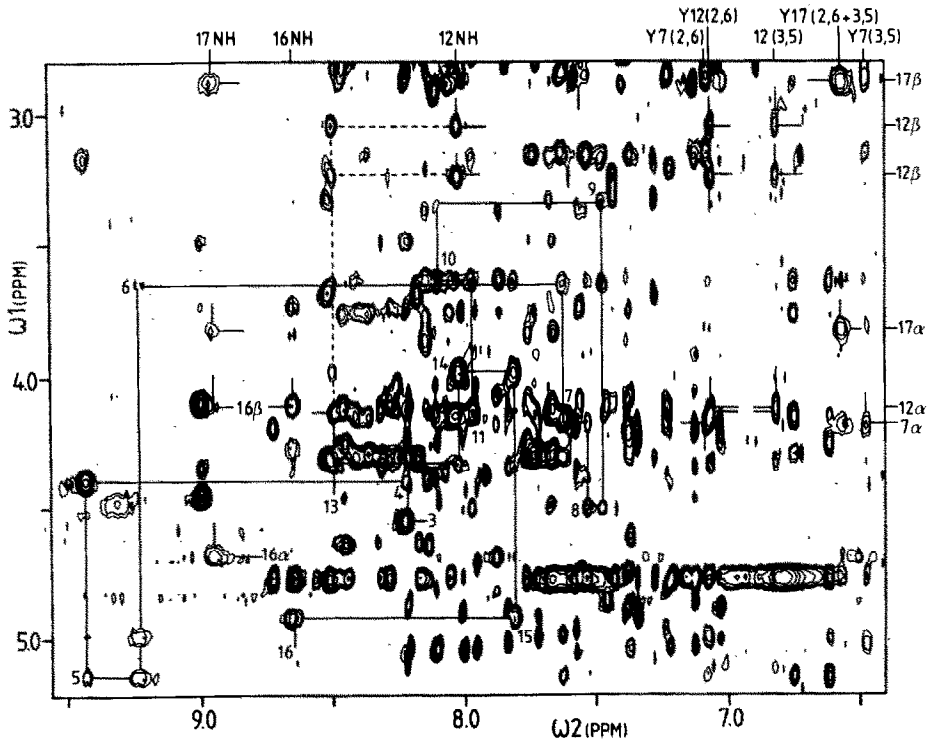

Fig. 3. Expanded region from $\omega_2 = 7.40$ to 9.56 ppm and $\omega_1 = 2.81$ to 5.21 ppm of the same spectrum as in Fig. 2. The sequential assignment of the protein segment from Pro 3 to Tyr 17 is shown, using the C^α-amide proton connectivities. The resonance positions of the aromatic residues are indicated. For more details see text.

operator complex in H_2O. It can be seen that there are only a few windows in the spectrum where only protein protons resonant. Conversely, there is only one region (5.2 to 6.5 ppm) where DNA protons do not overlap with those of the protein. Figure 3 shows an expanded view of the protein fingerprint region, where the C^αH-NH cross-peaks are located. The backbone proton assignments for the peptide region Pro 3 to Tyr 17 are indicated with lines connecting the intraresidue $d_{\alpha N}(i,i)$ cross-peaks with those corresponding to the sequential $d_{\alpha N}(i,i+1)$ ones. These assignments were obtained by a comparison of 2D NOE and 2D HOHAHA spectra of the complex taken at various salt concentrations.

Starting in the lower corner, the intraresidue cross-peak of Thr 5 is found, for which the C^α and amide protons have extreme low field shift values both in the complex and in the free headpiece. A vertical line connects with the C^αH of Val 4 and so on to Pro 3. The amide proton of Leu 6 could also be found easily. The resonance position of the amide proton of Tyr 7 is found via the aromatic resonances of this residue and the sequential amide-C^α proton cross-peak to Leu 6 in the following way. The exact position of the C^α proton of Tyr 7 is found using the cross-peaks between the C^α proton and the aromatic C2,6 and C3,5 protons, as indicated in Fig. 3. The sequential NOE to Asp-8 could then be identified and the sequential path up to Glu 11 can be followed easily. Because of overlap, both the intraresidue cross-peak between the amide and C^α protons of Tyr 12 and the sequential one to Glu 11 cannot be assigned. However, the C^α and C^β protons of Tyr 12 can again be found on the aromatic lines (Fig. 2), and the sequential steps from the amide proton of Ala 13, the position of which was initially based on a comparison with the free headpiece, gave the correct assignment of these two residues. Continuing at Ala 13, first Gly 14 (with two equivalent C^α proton resonances) and then Val 15 are found easily.

The resonance frequency of the amide of Ser 16 is found via the sequential cross-peak to the C^α proton of Val 15 and from the amide–amide connectivities to both Val 15 and Tyr 17 (not shown). Since the intraresidual cross-peaks of the amide proton of Ser 16 appear to be missing, these protons were assigned as follows. The amide proton of Tyr 17 has two additional cross-peaks which may belong to the C^α proton and one of the C^β protons of Ser 16. Evidence for this assignment came from a comparison of 2D NOE spectra recorded at increasing salt concentrations (see Fig. 4). At 1.2 M KCl most protons have the same chemical shift as in the free headpiece. The only exception is Gln 18, the amide proton of which is already shifted 0.13 ppm upfield indicative of some residual binding. At high salt the protons of Ser 16 can be assigned in the same way as in the free headpiece and the intraresidual cross-peaks remain present at 0.35 M KCl. The changes in chemical shift of C^α and C^β protons as a function of the salt concentration are shown in Fig. 4. The chemical shift values at 0.2 M KCl are measured for the sequential

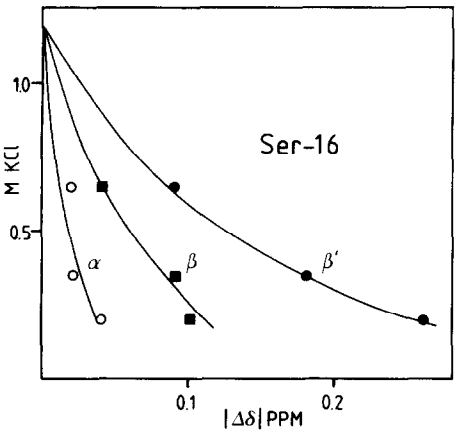

Fig. 4. Chemical shift of the C^{α} and C^{β} protons of Ser 16 in the HP56–11 bp complex as a function of concentration of KCl. The difference from the high salt (1.2 M KCl) is shown. The curves were used to assign these protons in the complex at low salt (0.2 M KCl). For more details see text.

cross-peaks on the amide of Tyr 17. As can be seen in Fig. 4, these values fit very well on the curves and thus confirm the resonance positions of the C^{α} and C^{β} protons of Ser 16 in the complex at 0.2 M KCl. Similarly, for the correct assignment of most residues of the recognition helix (17–25) and the loop region (26–33) many protons had to be followed in the salt titration.

Most proton resonances of residues belonging to helix III are shifted only slightly in the complex. The reason for this is that helix III is not involved in DNA binding. Because many C^{α} protons of this part of the protein overlap either with other C^{α} protons or with the H4′, H5′ and H5″ protons of the DNA, the sequential assignment via C^{α}H-amide connectivities was impossible. Instead, the assignment of this peptide segment could be made using the amide–amide pathway (not shown), which is very similar to that in the free headpiece. The assignment of the protons of Tyr 47 was made via the aromatic resonances of this residue in the same way as for the other tyrosines. Asn 46 and Ile 48 were then found easily.

In the free HP56, sequential assignment was only possible up to Arg 51. Subtraction of the 1D spectra of HP56 and HP51 showed that the protons of the remaining C-terminal residues resonate at random coil frequencies. From this it was concluded that the mobility of the C-terminal residues of unbound HP56 is such that they give no NOE build-up in the 2D spectra. However, in the complex the overall tumbling rate is lower and NOE cross-peaks are detectable for the protons of a few of these C-terminal residues, i.e. Val 52 and Ala 53. Again the protons of these residues resonate at random coil frequencies. Furthermore, if the salt concentration is raised, the NOE cross-peaks disappear again. These observations, together with the fact that the resonances belonging to Val 52 and Ala 53 have the smallest linewidth, suggest that also in the complex the C-terminal residues of the headpiece are more mobile than the rest of the protein. The amide proton of Lys-2 and the C^{α} proton of Met 1 could be assigned because they resonate at the same frequency as in the free headpiece.

Except for the three C-terminal amide protons and the one of Gln 18 which is too broad, all backbone amides could be assigned in the complex. Figure 5 shows the chemical shift differences these amide protons undergo upon complex formation. Some of these shifts can be explained by the proximity of the DNA. Thus, the amides of Leu 6, Ala 27 and Ser 31 are likely to be involved in hydrogen bonding with the phosphates. The origin of the shift of Val 24 is not clear.

Side chain amide resonances could also be assigned in the complex from following the intra-amide cross-peaks in a salt titration. Only that of Asn 25 shows a pronounced shift again correlated with hydrogen bond formation. Somewhat surprisingly the side chain amide protons of Gln 18, a residue in the recognition helix, do not display any DNA-induced shifts. One of these protons, however, shows an NOE to the H5 proton of cytosine 7.

Secondary structure of HP56 in the complex. A summary of the short and medium range NOEs observed in the HP56–11 bp operator complex is shown in Fig. 6. Comparison with previous results obtained for the free headpiece [20] shows that the present data are less complete but still sufficient to define the secondary structure of HP56 in the complex as virtually the same as in the free state.

Clearly, helix I is formed by residues 6–13, the same position as in unbound protein. In the free headpiece helix II is from Tyr 17 to Asn 25. In the complex several medium range NOEs between these residues are assigned but, due to the broadening of the amide proton resonance of Tyr 17 and the absence of the amide of Gln 18, medium range NOEs with these residues could not be identified. However, NOEs between the C^{α} proton of Tyr 17 and the methyl protons of Val 20 are present in both the complex and the free headpiece, and the same is true for all NOEs involving the aromatic protons of Tyr 17. From this we conclude that also in the complex Tyr 17 is the first residue of helix II and that it extends to Asn 25. The medium range NOE between Val 23 and Ala 27 shows that the loop region following helix II could be folded in very much the same way as in the free headpiece. Finally, for the third helical region nearly the same set of medium range NOEs is present in both the complex and in the free headpiece. Therefore, helix III is formed by residues 34–45.

Protein–DNA interaction

Information about the interaction of a protein with DNA can, in principle, be obtained from chemical shifts and from NOEs. The interpretation of chemical shift changes, however, is not unambiguous, and we use this information only in a qualitative sense. By contrast, the observation of an NOE between assigned protons is a measure of proximity and with a large number of NOEs the structure of macromolecular complexes can be obtained.

NOEs between headpiece and operator. Analysis of the 2D NOE spectra of complexes of HP56 with 11, 14 and 22 bp operator fragments in D_2O solution

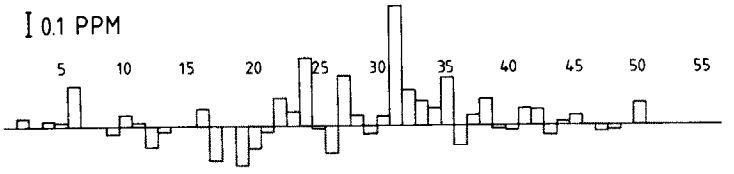

Fig. 5. Changes in proton chemical shift of the amide protons of HP56 induced by binding to the 11 bp half-operator. The differences are between the chemical shifts at 1.2 M KCl and those at 0.2 M KCl.

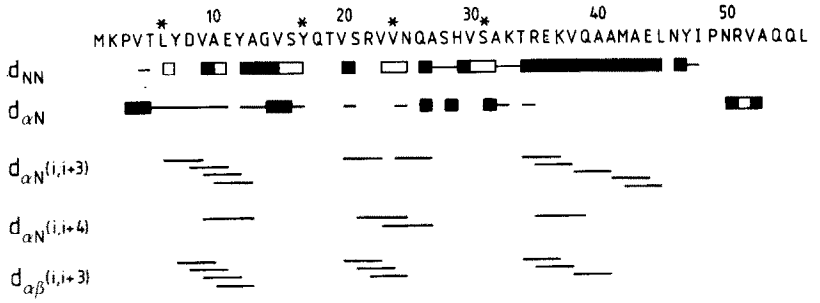

Fig. 6. Summary of the sequential and medium range NOEs of HP56 in the complex with the 11 bp operator. The thickness of the lines for the sequential NOEs correlated with the intensity of the NOE. The open bars indicate NOEs for which the intensities could not be characterized as strong or weak due to broadening or the fact that the cross-peak is close to the diagonal. The asterisks indicate amide proton resonances, which show substantial broadening.

[14, 15] showed that *ca.* 25 protein–DNA NOEs could be identified for each complex. The sets of NOEs are not identical for the three complexes, but in each case differences could be traced back to different overlap situations [15]. Therefore, essentially the same complex is formed with the three DNA fragments. It is interesting to note that this is true for the 22 bp operator complexed with two headpieces. Here the possibility of protein–protein interaction exists, although thus far no indication for cooperative binding have been found.

The 2D NOE spectra of the HP56–11 bp operator complex in H_2O yielded a few more protein–DNA NOEs involving exchangeable protons. We mentioned already the NOE cross-peak found between the side chain amide proton of Gln 18 and the H5 proton of base C7. This is an important NOE, because Gln 18 is implicated in the recognition of GC7 in genetic studies using the so-called "loss of contact" method [21]. The side chain amide protons could be easily followed in the salt titration, so that their assignment is unambiguous. Another NOE involving exchangeable protons is the one between the cytosine amino protons of GC9 with the aromatic protons of Tyr 17 (δ and ε-protons of Tyr 17 overlap in the complex). This confirms the proximity of Tyr 17 with GC9, since previously NOEs between the aromatic protons of this residue with the H5 and H6 protons of C9 had been formed.

The complete up-dated list of protein–DNA NOEs observed for HP56 complexes with various *lac* operator fragments is shown in Table 1. Note that in the table the distinction has been made between "unambiguous" and "probable" NOEs. This has been done because in the extremely crowded 2D NOE spectra (especially those taken in H_2O) it is sometimes difficult to rigorously exclude the possibility of assignment errors due to overlap. The "unambiguous" NOEs are all found at unique non-overlapping resonance positions, both for the protein and DNA protons. The "probable" ones are in crowded regions of the spectrum. However, these NOEs have been checked many times in various spectra and under various conditions, so that we consider the possibility of errors in assignment remote.

Structure of lac *headpiece–operator complex.* A structural model of the *lac* headpiece–operator complex was obtained as follows. From chemical shift and NOE considerations we had concluded that both headpiece and operator change their conformations only slightly upon binding. Therefore, we started modeling the complex using the NOE information, while keeping the operator in a standard B-DNA conformation and the headpiece in its NMR-derived structure [12]. Since the 2D NOE spectra were taken under conditions of limited spin diffusion, the upper bound distance constraints for the weak NOEs were set at the rather long distance of 6 Å. For the strong NOEs the upper bound was taken as 4 Å. Where necessary, pseudo-atom corrections were applied. Some of the side amino acid side chains in the DNA binding region of the headpiece were allowed to change their conformation. Models for the HP56-operator were then built, first on a graphics display system and later using the so-called ellipsoid algorithm [22]. Energy minimization of this model ensured that it had reasonable non-bonded interactions. After restrained molecular dynamics refinement [22] a model of the complex was obtained (shown in Fig. 7), in which all protein–DNA NOE constraints

Table 1. NOEs observed between *lac* headpiece and *lac* operator

Protein		DNA	
Unambiguous*			
Thr 5	$C^{\beta}H$	-G10	H3′
Leu 6	$C^{\delta}H_3$	-C9	H5
Tyr 7	H3,5	-G10	H8
Tyr 7	H2,6	-G10	H8
Tyr 7	H3,5	-G10	H1′†
Tyr 7	H3,5	-G10	H3′
Tyr 7	H3,5	-C9	H5
Tyr 7	H3,5	-C9	H6
Tyr 17	H3,5 + H2,6	-C9	H5
Tyr 17	H3,5 + H2,6	-C9	H6†
Tyr 17	H3,5 + H2,6	-T8	H6
Ser 21	$C^{\alpha}H$	-T8	H6
His 29	H2	-A2	H8†
His 29	H2	-T3	CH_3
His 29	H2	-A2	H1′‡
Probable*			
Thr 5	$C^{\gamma g}H_3$	-G10	H8
Thr 5	$C^{\gamma}H_3$	-G10	H3′
Leu 6	$C^{\delta}H_3$	-C9	H5
Leu 6	$C^{\delta}H_3$	-C9	H6
Leu 6	$C^{\delta}H_3$	-C9	H3′†
Leu 6	$C^{\delta}H_3$	-T8	H6†
Tyr 7	H3,5	-GC9	CH41†
Tyr 17	H3,5 + H2,6	-T8	CH_3
Tyr 17	H3,5 + H2,6	-GC9	CH41
Gln 18	$N^{\varepsilon}H_2$	-C7	H5
Ser 21	$C^{\alpha}H$	-T8	CH_3
Ser 21	$C^{\beta}H$§	-T8	CH_3
Ser 21	$C^{\beta}H$§	-T8	H6
Ser 21	$C^{\beta'}H$§	-T8	H6
His 29	H2	-A2	H3′
His 29	H2	-A2	H4′
His 29	H2	-A2	H5′§
His 29	H2	-A2	H5″§
His 29	H4	-T3	CH_3
His 29	H4	-T4	CH_3
His 29	H2	-T4	CH_3
His 29	$C^{\beta}H$§	-T4	H6
His 29	$C^{\beta'}H$§	-T4	H6
His 29	$C^{\beta}H$§	-T3	H6
His 29	$C^{\beta'}H$§	-T3	H6

* Unambiguous NOEs were assigned at unique resonance frequencies. Probable NOEs were from resonances in crowded spectral regions, where there is some uncertainty of assignment (see text for discussion).

† Due to overlap these NOEs could not be identified in the spectra of the 11 bp complex. These NOEs were assigned from spectra of the HP56–14 bp complex.

‡ Assigned in the complex of HP56 and a 22 bp symmetric operator.

§ H5′ and H5″ protons, C^{β} and $C^{\beta'}$ protons were only pairwise assigned.

could be satisfied simultaneously. This is important because it virtually excludes the possibility that some of the observed NOEs are due to non-specific complexes. Although these are certainly formed at the high concentrations (5 mM) of the NMR experiments, they do not lead to observable NOEs (inconsistent with the specific complex), most likely because their lifetime is not long enough to allow build-up of NOE intensity.

The most surprising feature of the model is that the orientation of the second or "recognition" helix in the major groove of DNA with respect to the dyad axis at GC11 is opposite to what is found in all other models of repressor–operator interaction, either from direct X-ray observation [3–5, 7] or from models built for CAP and λ and cro repressors [23]. Indeed, it is also opposite to orientations predicted for *lac* repressor on the basis of the analogy of models for CAP [24] and cro repressor [25]. In these models the first helix would be away from the dyad axis, while in the complex shown in Fig. 7 it is close to it. One of the strongest protein–DNA NOEs is that between the (overlapping) ring protons of Tyr 17 and the 5-methyl group of T8. It suggests that this is a functional contact since it is known that the T8 methyl group is essential for repressor binding [26].

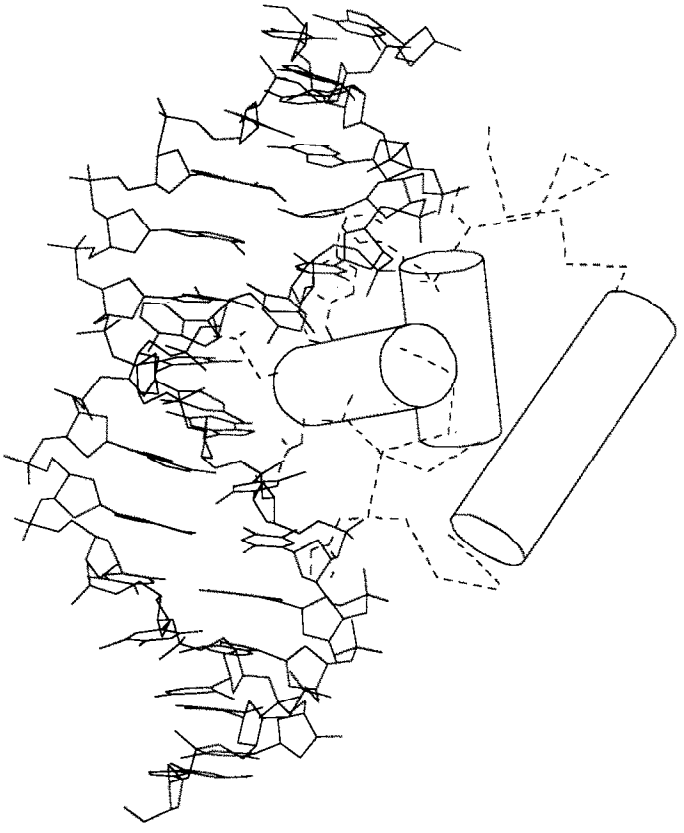

Fig. 7. Structure of the headpiece–operator complex obtained by docking and restrained molecular dynamics refinement using NOE based distance constraints.

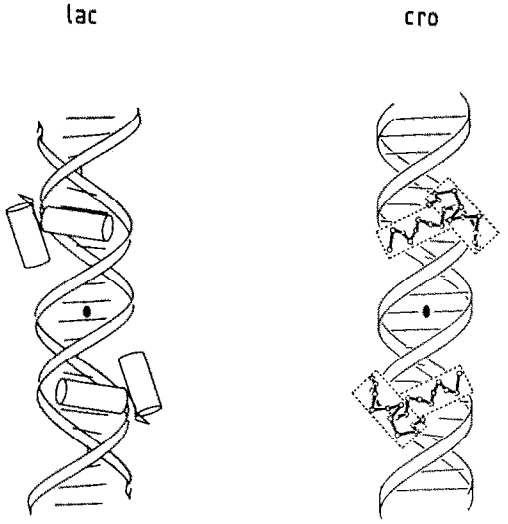

Fig. 8. Helix-turn-helix domain in repressor–operator complexes for *lac* repressor as determined from NMR and as proposed for cro (taken from Ref. 23). The orientation of the recognition helix is approximately opposite in both models. Note that in the *lac* repressor–operator model this helix is almost perpendicular to the DNA helix axis, while in the proposed cro model it lies more parallel to the direction of the major groove.

An important question is whether the whole *lac* repressor binds to the operator with its headpieces in the same orientation as we have found for isolated headpieces. Recently, genetic experiments carried out in the laboratory of B. Müller-Hill have shown that this is actually the case. A *lac* repressor mutant was constructed with the first two amino acids of the recognition helix replaced by those of the *gal* repressor (Tyr 17 → Val, Gln 18 → Ala). This mutant repressor had high affinity for the *gal* operator, which differs from the *lac* operator at positions 7 and 9. Although this already gives some clue as to the orientation of the recognition helix, a more definitive result was their finding of a repressor mutant with Arg 22 replaced by His, which now had specificity for a *lac* operator with GC5 replaced by TA [16]. This provides support for the Arg 22-GC5 contact in the native system, that we predicted based on our NMR results [14]. It also fixes unambiguously the orientation of the recognition helix as opposite to that of cro and λ repressors. These different modes of binding of the helix-turn-helix motif on the operators are shown in Fig. 8. It appears, therefore, that there are two classes of helix-turn-helix proteins, which can be generically designated as *lac* and cro. From homology arguments and also based on the genetic experiments [16] it appears that at least the *gal* and *deo* repressors belong to the *lac* class. The repressors with known crystal structures, λ cI, cro,

trp, 434 (and the related P 22) and also CAP, fall in the cro class.

REFERENCES

1. von Hippel PH and McGhee JD, DNA–protein interactions. *Annu Rev Biochem* **41**: 231–300, 1972.
2. Seeman NC, Rosenberg JM and Rich A, Sequence specific recognition of double-helical nucleic acids by proteins. *Proc Natl Acad Sci USA* **73**: 804–808, 1976.
3. Jordan SR and Pabo CO, Structure of the lambda complex at 2.5 Å resolution: Details of repressor–operator interactions. *Science* **242**: 893–899, 1988.
4. Aggarwal AK, Rodgers DW, Drottar M, Ptashne M and Harrison SC, Recognition of a DNA operator by the repressor of phage 434: A high resolution view. *Science* **242**: 899–907, 1988.
5. Wolberger C, Dong Y, Ptashne M and Harrison SC, Structure of a phage 434 Cro/DNA complex. *Nature* **335**: 789–795, 1988.
6. Harrison SC, Anderson JE, Koudelka GB, Mondragon A, Subbiah S, Wharton RP, Wolberger C and Ptashne M, Recognition of DNA sequences by the repressor of bacteriophage 434. *Biophys Chem* **29**: 31–37, 1988.
7. Otwinowski Z, Schevitz RW, Zhang R-G, Lawson CL, Joachimiak A, Marmorstein RQ, Luisi BF and Sigler PB, Crystal structure of *trp* repressor/operator complex at atomic resolution. *Nature* **335**: 321–329, 1988.
8. McKay DB and Steitz TA, Structure of catabolite gene activator protein at 2.9 Å resolution suggests binding to left-handed B-DNA. *Nature* **290**: 744–749, 1981.
9. Pabo CO and Lewis M, The operator-binding domain of λ repressor: Structure and DNA recognition. *Nature* **298**: 443–447, 1982.
10. Anderson WF, Ohlendorf DH, Takeda Y and Matthews BW, Structure of the cro repressor from bacteriophage λ and its interaction with the DNA. *Nature* **290**: 754–758, 1981.
11. Zuiderweg ERP, Kaptein R and Wüthrich K, Secondary structure of the *lac* repressor DNA-binding domain by two-dimensional ^{1}H nuclear magnetic resonance in solution. *Proc Natl Acad Sci USA* **80**: 5837–5841, 1983.
12. Kaptein R, Zuiderweg ERP, Scheek RM, Boelens R and van Gunsteren WF, A protein structure from nuclear magnetic resonance data. *lac* Repressor headpiece. *J Mol Biol* **182**: 179–182, 1985.
13. Kaptein R, Boelens R, Scheek RM and van Gunsteren WF, Protein structures from NMR. *Biochemsitry* **27**: 5389–5395, 1988.
14. Boelens R, Scheek RM, van Boom JH and Kaptein R, Complex of *lac* repressor headpiece with a 14 base-pair *lac* operator fragment studied by two-dimensional nuclear magnetic resonance. *J Mol Biol* **193**: 213–216, 1987.
15. Lamerichs RMJN, Boelens R, van der Marel GA, van Boom JH, Kaptein R, Buck F, Fera B and Rüterjans H, ^{1}H NMR study of a complex between *lac* repressor headpiece and a 22 base pair symmetric *lac* operator. *Biochemistry* **28**: 2985–2991, 1989.
16. Sartorius J, Lehming N, Kisters B, von Wilcken-Bergmann B and Müller-Hill B, *lac* Repressor mutants with double or triple changes in the recognition helix bind specifically to *lac* operator variants with multiple exchanges. *EMBO J* **8**: 1265–1270, 1989.
17. Wüthrich K, *NMR of Proteins and Nucleic Acids*. John Wiley, New York, 1986.
18. Hare DR, Wemmer DE, Chou SH, Drobny G and Reid BR, Assignment of the non-exchangeable proton resonances of d(CGCGAATTCGCG) using two-dimensional NMR methods. *J Mol Biol* **171**: 319–336, 1983.
19. Scheek RM, Russo N, Boelens R and Kaptein R, Sequential resonance assignments in DNA ^{1}H NMR spectra by two-dimensional NOE spectroscopy. *J Am Chem Soc* **105**: 2914–2916, 1983.
20. Zuiderweg ERP, Scheek RM and Kaptein R, Two-dimensional ^{1}H NMR studies on the *lac* repressor DNA binding domain: Further resonance assignments and identification of nuclear Overhauser enhancements. *Biopolymers* **24**: 2257–2277, 1985.
21. Ebright RH, Use of "loss-of-contact" substitutions to identify residues involved in an amino acid-base pair contact. *J Biomol Struct Dyn* **3**: 281–297, 1985.
22. Rullmann JAC, Boelens R and Kaptein R, NMR based docking studies of *lac* repressor headpiece on a *lac* operator fragment. In: *DNA–Protein Interactions in Transcription* (Ed. Gralla JD), pp. 11–24. Alan R. Liss, New York, 1989.
23. Pabo CO and Sauer RT, Protein–DNA recognition. *Annu Rev Biochem* **53**: 293–321, 1984.
24. Weber IT, McKay DB and Steitz TA, Two helix DNA binding motif of CAP found in *lac* repressor and *gal* repressor. *Nucleic Acids Res* **10**: 5085–5094, 1982.
25. Matthews BW, Ohlendorf DH, Anderson WF and Takeda Y, Structure of the DNA binding region of *lac* repressor inferred from its homology with cro repressor. *Proc Natl Acad Sci USA* **79**: 1428–1432, 1982.
26. Caruthers MH, Deciphering the protein–DNA recognition code. *Acc Chem Res* **134**: 155–160, 1980.